

Contact calculation and simulation analysis of the involute cylindrical gear

Lü Hongzhan Hou Zhiyong Wang Junzheng Wang Yuda

(College of Mechanical Engineering, Donghua University, Shanghai 201620, China)

Abstract: To facilitate the contact analysis of involute cylindrical gears, a meshing contact analysis and tooth profile modification algorithm program for involute cylindrical gears is designed. The involute spur gear parameter equation is employed to accurately model the radius of curvature of the tooth profile contact point, and the Hertz contact formula is enhanced to solve the gear meshing contact stress considering the actual load. To reduce the impact of gear meshing, five tooth profile modification methods and their contact stress analysis methods after modification are given in the algorithm program. Compared with the calculations by MASTA, the industry-recognized gear design simulation software, the algorithm program has a higher accuracy in solving the contact stress and the contact stress distribution after tooth profile modification accords with the MASTA calculation results, and the average error is about 5.04%, which confirms the rationality of the algorithm program.

Key words: involute cylindrical gear; Hertz formula; contact analysis; program development

DOI: 10.3969/j.issn.1003-7985.2024.01.008

Involute spur gear transmission is one of the fundamental forms of mechanical transmissions. It is extensively employed in the transmission parts of different automatic equipment because of its constant instantaneous drive ratio, compact structure, and stable power transmission. Calculations and analysis of gear contact play an important role in the assessment of transmission quality in the development of gear transmission^[1].

During the gear contact analysis, modeling the meshing gear pair is a preprocessing work of the contact analysis. The modeling methods for standard involute tooth profiles are now mature; for the modeling of modified nonstandard involute gears and racks, Zhai et al.^[2] suggested a novel parametric modeling method for spur gears, which achieved parametric modeling and optimization of the involute spur gear curve using Scilab software. Chen et

al.^[3] researched the geometric design of pure rolling racks and pinion mechanisms by simulation and stress analysis and proposed a design method for pure rolling meshing, which can reduce the relative sliding between the tooth surfaces and has better mechanical performance than standard gears and racks. All of these works provide applied and theoretical references for modeling involute gears.

Several factors are involved in calculations of gear contact stress, and extensive research has been conducted on involute gear transmission. Vouaillat et al.^[4] examined the rolling contact fatigue of spur gears in terms of material micromechanics. A fatigue criterion based on rolling contact fatigue microcrack nucleation at grain boundaries is proposed by analysis of the materials and local microscopic geometry. Wen et al.^[5] developed a multidegree-of-freedom analysis and calculation model that considers misalignment errors, which can accurately and quickly compute the tooth surface contact stress distribution of gear pairs with misalignment errors in multiple degrees of freedom. Sivayogan et al.^[6] studied the contact analysis of spur gears of high-performance transmission systems based on lubrication load. Lubricated Loaded Tooth Contact Analysis based on thermal elastohydrodynamic lubrication was proposed, which considers the effect of tooth surface lubrication and makes the analysis closer to the actual conditions. Many studies have shown that the periodic meshing of the involute cylindrical gear can be approximated as Hertz contact^[7], and the contact stress between the two tooth surfaces can be determined using the modified Hertz formula and other conditions that must be considered simultaneously during the transmission. The finite element method is commonly utilized to compute the contact stress, which can effectively analyze the gear contact problem and satisfy the engineering accuracy requirements. However, the mainstream finite element codes are developed commercially and thus are expensive and technically not very suitable for computational analysis of gear mesh contacts.

During the standard and unmodified cylindrical gear transmissions, due to the presence of alternate meshing areas of a single tooth and double teeth, sudden changes in the contact stress are observed at the area of the transition between the single tooth and double teeth meshing areas, which leads to instantaneous meshing shock and op-

Received 2022-06-27, **Revised** 2023-12-15.

Biography: Lü Hongzhan (1979—), male, doctor, associate professor, lvhz@dhu.edu.cn.

Foundation item: The National Key Research and Development Program of China (No. 2018YFB2001702).

Citation: Lü Hongzhan, Hou Zhiyong, Wang Junzheng, et al. Contact calculation and simulation analysis of the involute cylindrical gear[J]. Journal of Southeast University (English Edition), 2024, 40(1): 68 – 79. DOI: 10.3969/j.issn.1003-7985.2024.01.008.

erating noise and affects the smoothness and reliability of gear meshing. For the above problem, gear tooth modifications of standard involute gears are usually employed. In-depth explorations of the influence of gear tooth modification on the load distribution coefficient, meshing stiffness, contact stress, and other parameters have been conducted. To reduce gear tooth failure due to surface pitting or root fracture, Maper et al.^[8] researched the enhancement of gear contact by tip relief and other gear profile modifications (PMs) and derived formulas to estimate contact and bending stresses. Pleguezuelos et al.^[9] identified the influence of symmetrical long tooth profile modifications on the quasistatic transmission error of high-contact-ratio spur gears. A previously developed model for the load-sharing ratio and quasistatic transmission error was employed to acquire tip reliefs for the minimum peak-to-peak amplitude of the quasistatic transmission error and for the minimum dynamic load. Considering the spur gears operating in mixed elastohydrodynamic lubrication, Kimiaei and Akbarzadeh^[10] suggested a conceptual model based on load-sharing theory. They studied the influence of tip relief on the performance of spur gears, the amount of wear, and the lubricant film thickness. These studies offer theoretical support for examining the modification methods of involute cylindrical gears, but this is not easy to achieve in engineering.

This paper is structured as follows. The first part focuses on the realization of gear parametric modeling based on the generating method, which provides models for subsequent calculation and analysis. The second part describes the theory and methodology of involute spur gear contact stress calculation and expression. The third part presents the methods of tooth profile modification. Finally, we verify and evaluate the proposed methods by com-

paring the results of the algorithm program with the MASTA results. The process presented in the manuscript provides a convenient contact stress calculation and result visualization procedure for the meshing analysis of involute cylindrical gears.

1 Modeling of Involute Spur Gears

1.1 Principle of gear parametric modeling based on the generating method

Parametric equations are utilized to model the tooth profile piecewise under a Cartesian coordinate system, and the main parts include the addendum profile, dedendum profile, involute profile, and dedendum transition fillet profile.

According to the standard rack structure, the processing principle of generating method of the involute spur gear is shown in Fig. 1, and the coordinate transformation matrix \mathbf{M} is shown as follows^[11]:

$$\mathbf{M} = \begin{bmatrix} a_{11} & a_{12} & a_{13} \\ a_{21} & a_{22} & a_{23} \\ a_{31} & a_{32} & a_{33} \end{bmatrix} \quad (1)$$

where $a_{11} = \cos\lambda$, $a_{12} = \sin\lambda$, $a_{13} = (d - m) \sin\lambda - vt\cos\lambda$, $a_{21} = -\sin\lambda$, $a_{22} = \cos\lambda$, $a_{23} = (d - m) \cos\lambda + vt\sin\lambda$, $a_{31} = a_{32} = 0$, $a_{33} = 1$, and $\lambda = \omega t$; m is the module of the gear; $d - m$ is the distance between the origin of the coordinate system $O_1X_1Y_1$ and the point O_2 ($d = m(z/2 + x)$, where z is the number of teeth and x is modification coefficient). The tooth profile equations of each segment in the gear coordinate system $O_2X_2Y_2$ are obtained. Eq. (2) is the parametric equation of the involute:

$$\left. \begin{aligned} X_{AB2} &= \frac{1}{1 + \tan^2\alpha} \left[(\tan\alpha \sin\lambda + \cos\lambda) \left(\frac{\pi}{4}m - \frac{mz\lambda}{2} + d\tan\alpha \right) - (\tan\alpha \cos\lambda - \sin\lambda) \frac{mz}{2} \right] \\ Y_{AB2} &= \frac{1}{1 + \tan^2\alpha} \left[(\tan\alpha \cos\lambda - \sin\lambda) \left(\frac{\pi}{4}m - \frac{mz\lambda}{2} + d\tan\alpha \right) + (\tan\alpha \sin\lambda + \cos\lambda) \frac{mz}{2} \right] \end{aligned} \right\} \quad (2)$$

where α is the pressure angle. Eq. (3) is the parametric equation of the addendum and root circles, and Eq. (4) is the parametric equation of the dedendum transition fillet.

$$\left. \begin{aligned} x_a &= r_a \cos\varphi, \quad y_a = r_a \sin\varphi \\ x_f &= r_f \cos\varphi, \quad y_f = r_f \sin\varphi \end{aligned} \right\} \quad (3)$$

where r_a is the addendum radius; r_f is the dedendum radius; φ is the rotation angle of the involute spur gear.

$$\left. \begin{aligned} X_{BC2} &= Z_1 - \frac{0.38mZ_4}{\sqrt{Z_2^2 + Z_4^2}} \\ Y_{BC2} &= Z_3 + \frac{0.38mZ_2}{\sqrt{Z_2^2 + Z_4^2}} \end{aligned} \right\} \quad (4)$$

where

$$\begin{aligned} Z_1 &= (a - r\lambda) \cos\lambda + b \sin\lambda, \quad Z_2 = (b - r) \cos\lambda + (r\lambda - a) \sin\lambda \\ Z_3 &= (r\lambda - a) \sin\lambda + b \cos\lambda, \quad Z_4 = (r - b) \sin\lambda + (r\lambda - a) \cos\lambda \end{aligned}$$

where $r = 0.38m$.

In Fig. 1, the rack moves toward the negative X_1 direction with a v speed in its coordinate system. The gear blank rotates around the center O_2 of the circle at an angular velocity ω . Regarding the coordinate $O_2X_2Y_2$ as the reference coordinate system, the rack translation is transformed to pure rolling around the coordinate origin O_2 (the center of the gear). The line segment AB is the part of the rack tooth profile that can generate the involute part of the gear tooth profile. The segment BC can generate

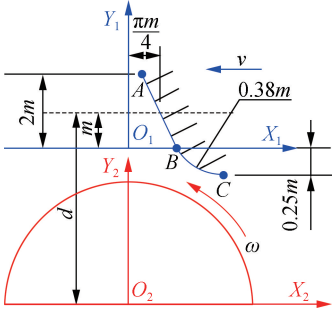


Fig. 1 Coordinates of the rack cutting the gear blank by the generating method

part of the tooth root transition fillet.

The involute tooth profile is obtained through the above parametric equations when the value intervals of the independent variables of each segment's tooth profile parametric equations are determined, as shown in Fig. 2. The value intervals can be solved using Eq. (5).

$$\left. \begin{aligned} \theta &= \frac{2\pi}{z} \\ \theta_{\text{invl}} &= \tan\left(\arccos \frac{r_b}{r}\right) - \arccos \frac{r_b}{r} \\ \theta_{\text{inv}} &= \tan\left(\arccos \frac{r_b}{r_a}\right) - \arccos \frac{r_b}{r_a} \\ \theta_a &= \frac{\theta}{4} + \theta_{\text{invl}} - \theta_{\text{inv}} \end{aligned} \right\} \quad (5)$$

where θ_a is the half evolving angle of the addendum arc of a tooth; θ_{invl} is the evolving angle of the involute tooth profile of the half tooth; θ_{inv} is the evolving angle of the involute tooth profile of the half tooth below the reference circle; θ_f is the evolving angle of the tooth root arc of one side of a tooth; r is the radius of the reference circle; r_b is the radius of the base circle. θ_r and θ_f need to be solved by dichotomy and trichotomy. θ_a needs to be solved by dichotomy.

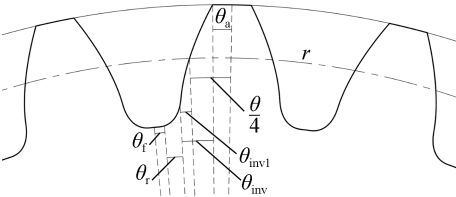
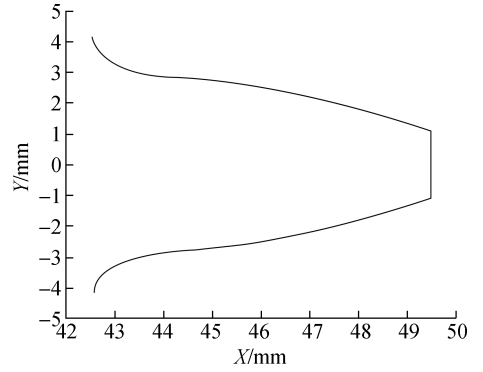


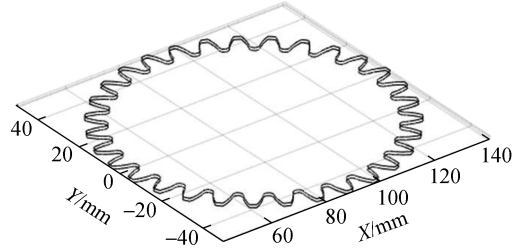
Fig. 2 Intervals of the tooth profile parametric equations of each segment

1.2 Case of gear modeling

Based on the equations above, the algorithm of parametric equation modeling is developed to generate the tooth profiles of single and all teeth of involute spur gears. The modeling results of the involute spur gear are illustrated in Fig. 3, where modulus $m = 3$ mm and number of teeth $z = 31$.



(a)



(b)

Fig. 3 Modeling results of the involute spur gear. (a) Modeling of a single tooth; (b) Modeling of all teeth

2 Theory and Method of Involute Spur Gear Contact Stress Calculation

2.1 Theory of involute spur gear contact stress calculations

The calculations of the spur gear contact stress are the basis of spur gear contact analysis, and in this work, the classical Hertz contact theory is adopted to solve the contact stress. Based on the Hertz contact theory, it is hypothesized that the contact stress of involute spur gears can be approximately calculated by cylindrical rollers instead. Here, two elastic cylinders, whose lengths are L_c and radii are R_1 and R_2 , are in contact with normal pressure, which results in elastic deformation. The initial state of the line contact becomes a surface contact under the force F_n , and the contact surface is a rectangle whose length is L and width is $2b$. From the elasticity theory, the width $2b$ of the contact area can be solved using Eq. (6).

$$2b = \sqrt{\frac{16F_t}{\pi L} \frac{(1 - \nu_1^2)/E_1 + (1 - \nu_2^2)/E_2}{1/\rho_1 + 1/\rho_2}} \quad (6)$$

where ν_1 and ν_2 are Poisson's ratios of materials; E_1 and E_2 are the elastic moduli of materials; ρ_1 and ρ_2 are the composite curve radii; F_t is the normal pressure. The contact stress σ of the involute spur gears at a certain moment can be derived as^[12]

$$\sigma = \sqrt{\frac{F_t}{\pi L} \frac{1/\rho_1 + 1/\rho_2}{(1 - \mu_1^2)/E_1 + (1 - \mu_2^2)/E_2}} \quad (7)$$

It can be observed from Eq. (7) that to determine the gear contact stress distribution, the radii of curvature of the tooth profile need to be calculated correctly. The radius of curvature of the tooth profile can be calculated using the equation of the radius of curvature in the form of a parametric equation:

$$k = \frac{x'y'' - x''y'}{(x'^2 + y'^2)^{3/2}} \quad (8)$$

Assuming that the curve is determined by an equation $y = f(x)$ that has the second order of derivative in a Cartesian coordinate system, $\tan\theta = y' = f'(x)$, and $\sec^2\theta \frac{d\theta}{dx} = y''$, based on the Euler-Savary equation (Eq. (9))^[13], the radius of curvature of the second gear tooth profile in the same coordinate system can be directly obtained.

$$\frac{1}{\rho_1 - r_D} + \frac{1}{\rho_2 + r_D} = \left(\frac{1}{r_1} + \frac{1}{r_2} \right) \frac{1}{\sin\phi} \quad (9)$$

where r_1 and r_2 are the radii of pitch circles; r_D is the distance of the straight line from the instantaneous contact point to the pitch point; ϕ is the angle between r_D and the common tangent of pitch circles.

2.2 Load distribution and correction coefficient

In a meshing circle of involute spur gears, there are situations where the meshing areas of single and double teeth alternately appear continuously. In theory, in a single-tooth meshing area, a pair of gear teeth bear almost all the loads; in a double-tooth meshing area, the gear tooth bears half the load, as marked by the dashed line $A_0B_0C_0D_0E_0F_0G_0H_0$ in Fig. 4. However, because of factors such as manufacturing, processing, and assembly errors, the alternate meshing areas of single and double teeth will cause deformations such as elastic deformation, shear deformation, and bending deformation, which makes the actual load distribution on the tooth surface of the involute spur gear participating in meshing almost follows the solid line $ABCDEFGH$ in Fig. 4.

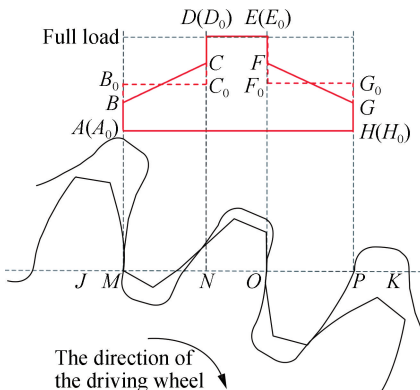


Fig. 4 Load distribution of a meshing circle of the involute spur gear

Because of the uneven load distribution, the Hertz contact equation cannot be employed directly to compute the gear contact stress. Otherwise, there will be a large deviation, and the changing load needs to be corrected. Based on the law of the load distribution in each meshing circle and the operating condition of the tooth surface, the value of the contact stress is fixed by introducing the load distribution coefficient $R(\varepsilon)$, as shown in Fig. 5^[14].

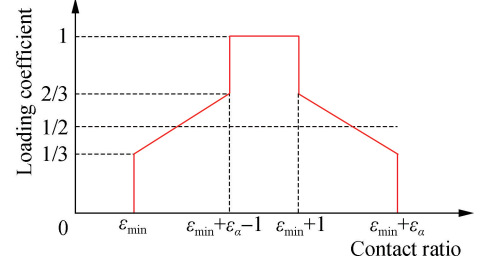


Fig. 5 Load distribution coefficient

Meanwhile, the effect of the actual operating conditions and other additional factors on the gears also should be considered when solving contact stress. Based on the standards of the ISO-6336 series^[15], the load correction coefficients should be added to the Hertz formula, including the application factor K_A , the dynamic factor K_v , the face load factor (contact stress) $K_{H\beta}$, and the transverse load factor (contact stress) $K_{H\alpha}$.

$$K_v = N(C_{v1}B_p + C_{v2}B_f + C_{v3}B_k) + 1 \quad (10)$$

where

$$B_p = \frac{c'f_{pbeff}b}{K_A F_t}, \quad B_f = \frac{c'f_{faeff}b}{K_A F_t}, \quad B_k = \left| 1 - \frac{c'C_a b}{K_A F_t} \right|$$

where f_{pbeff} refers to the effective extreme deviation of base pitch; c' refers to the stiffness of a tooth pair; b refers to the tooth width; f_{faeff} denotes the effective tooth profile tolerance; C_a refers to the design amount for profile modification (tip relief at the beginning and end of tooth engagement); N refers to the ratio of critical speed of rotation; F_t is the tangential load; C_{v1} allows for tooth pitch deviation effects, which is equal to 0.32; C_{v2} allows for tooth profile deviation effects, which is equal to 0.34; C_{v3} allows for the cyclic variation effect in mesh stiffness, which is equal to 0.23.

$$K_{H\beta} = 1 + \frac{4000}{3\pi} x_\beta \frac{c_\gamma}{E} \left(\frac{b}{d_1} \right)^2 \left[5.12 + \left(\frac{b}{d_1} \right)^2 \left(\frac{l}{b} - \frac{7}{12} \right) \right] + \frac{x_\beta c_\gamma f_{ma} b}{2F_m} \quad (11)$$

where l is the bearing span; f_{ma} is the mesh misalignment due to manufacturing deviations, with a rough value of 15 μm ; x_β is a running-in factor, with a value for a common material of 0.85; d_1 is the diameter of the reference circle; F_m is the mean transverse tangential load at the refer-

ence circle relevant to mesh calculations.

$$K_{H\alpha} = \frac{\varepsilon_\gamma}{2} \left[0.9 + 0.4 \frac{c_\gamma b (f_{pb} - y_\alpha)}{F_{tH}} \right] \quad (12)$$

where ε_γ is the total contact ratio; y_α is a running-in allowance for a gear pair, with a value for a common gear material of $0.075f_{pb}$; f_{pb} is the transverse base pitch deviation; F_{tH} is the determinate tangential load.

In summary, considering the operating conditions and load distribution factors, the revised Hertz contact equation is obtained as follows:

$$\sigma = K_A K_v K_{H\beta} K_{H\alpha} \sqrt{\frac{F_t R(\varepsilon)}{\pi L} \frac{1/\rho_1 + 1/\rho_2}{(1 - \mu_1^2)/E_1 + (1 - \mu_2^2)/E_2}} \quad (13)$$

2.3 Example of the calculation

Based on the theories above, the algorithm is developed to calculate the contact stress of involute spur gears when the basic parameters of the gears are input, namely, the modulus $m = 4$ mm, the numbers of teeth $z_1 = 30$ and $z_2 = 37$, the pressure angle $\alpha = 20^\circ$, the tooth width $b = 30$ mm, the clearance coefficient $c^* = 0.25$, the addendum coefficient $h_a^* = 1$, Poisson's ratio $\nu = 0.3$, the elastic modulus $E = 205$ GPa, the input power $P = 5$ kW, and the rotational speed $n = 1\,600$ r/min. The results of the contact stress of the unmodified involute spur gears are shown in Fig. 6, which initially achieves the visualization of the calculation and analysis of the contact stress of the involute spur gears. In Fig. 6, N denotes the number of discrete points of tooth profile.

3 Transmission Characteristics and Tooth Profile Modification of Involute Spur Gears

3.1 Principle of involute spur gear modification

Based on the analysis of the load distribution coefficient in the actual meshing process, there are several sudden changes in the load at the contact points in a meshing circle, as indicated by the dashed line $A_0B_0C_0D_0E_0F_0G_0H_0$ in Fig. 7. These sudden changes result in excessive local elastic deformation that can cause meshing interference. The tip relief is used to improve this problem. After the tip relief, the trend of the load distribution follows the black solid line $ADEH$, which decreases with sudden changes.

The driving and driven gears of the involute spur gears are modified by the tip relief method. The equation of the tip relief can be determined by calculating the maximum deformation and maximum modification of the tooth profile. Then, the contact stress distribution after modification is solved. Finally, the reliability of the algorithm can be proven by comparison with the results of the MASTA-generated tooth profile modification.

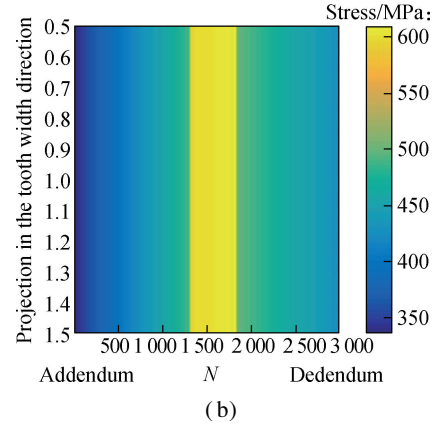
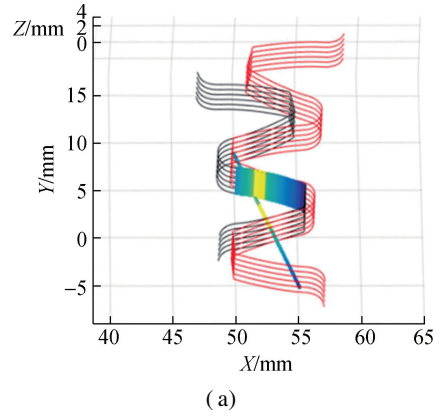


Fig. 6 Contact analysis of involute spur gears according to the algorithm. (a) Meshing load distribution; (b) Distribution of surface contact stress

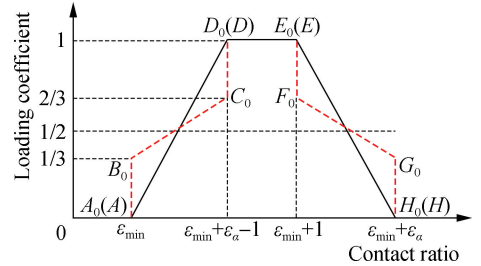


Fig. 7 Load distribution coefficients of unmodified and modified tooth profiles

3.2 Tip relief of involute spur gears

3.2.1 Maximum amount of modification

In the tip relief, selecting the maximum amount of modification should ensure that interference is avoided as much as possible when the tip of the gear tooth enters meshing. An excessive amount of tooth profile modification will cause discontinuous transmission and aggravate dynamic load, which is bad for transmission. The maximum amount of modification is equal to that of the elastic deformation of the tooth profile after being loaded plus 70% of that of elastic deformation (to allow for misalignment) plus the possible base (adjacent) pitch errors of $3\ \mu\text{m}$ on each gear and the possible profile errors of $3\ \mu\text{m}$ on each gear^[16]. According to the method recommended by the Japan Society of Mechanical Engi-

neers^[17], the total amount of elastic deformation of the tooth after being loaded Δ is determined by the deflections Δ_f of the tooth profile near the tooth root, the deflections Δ_{inv} of the involute tooth profile, the deflections Δ_s resulting from the shear stress, the deflections Δ_b resulting from the inclination of the basic part, and the deflections Δ_c of the contact area of the tooth surface, namely,

$$\Delta = \Delta_f + \Delta_{inv} + \Delta_s + \Delta_b + \Delta_c \quad (14)$$

where

$$\Delta_f = \frac{12F_t \cos^2 \alpha}{Ebs_F^3} \left[h_s h_r (h_s - h_r) + \frac{h_r^3}{3} \right] \quad (15)$$

$$\Delta_{inv} = \frac{6F_t \cos^2 \alpha}{Ebs_F^3} \left[\frac{h_i - h_s}{h_i - h_r} \left(4 - \frac{h_i - h_s}{h_i - h_r} \right) - 2 \ln \left(\frac{h_i - h_s}{h_i - h_r} \right) - 3 \right] \cdot (h_i - h_r)^3 \quad (16)$$

$$\Delta_s = \frac{2F_t \cos^2 \alpha (1 + \nu)}{Ebs_F} \left[h_r + (h_i - h_r) \ln \left(\frac{h_i - h_s}{h_i - h_r} \right) \right] \quad (17)$$

$$\Delta_b = \frac{24F_t \cos^2 \alpha h_s^2}{\pi Ebs_F^2} \quad (18)$$

$$\Delta_c = \frac{4F_t (1 - \nu^2)}{\pi Eb} \quad (19)$$

where s_F is the safety factor of tooth root bending failure (solved by Eq. (20)); r_F is the effective radius of the root circle (translated by Eq. (21)).

$$s_F = \begin{cases} 2r_F \sin \left(\frac{\pi + 4x \tan \alpha}{2z} + \text{inv}(\alpha) - \text{inv} \left(\arccos \left(\frac{r_b}{r_F} \right) \right) \right) & r_b \leq r_F \\ 2r_b \sin \left(\frac{\pi + 4x \tan \alpha}{2z} + \text{inv}(\alpha) \right) & r_b > r_F \end{cases} \quad (20)$$

$$r_F = r_b \sec \left(\arctan \left(\sqrt{\left(\frac{r_a}{r_b} \right)^2 - 1} \right) \right) \quad (21)$$

To simplify the calculation equation, the variables h_s , h_r and h_i are set, as shown in Eqs. (22)-(24).

$$h_s = d_x - \sqrt{r_f^2 - \frac{s_F^2}{4}} \quad (22)$$

$$h_r = \begin{cases} \sqrt{r_F^2 - \frac{s_F^2}{4}} - \sqrt{r_f^2 - \frac{s_F^2}{4}} & r_b \leq r_F \\ \sqrt{r_b^2 - \frac{s_F^2}{4}} - \sqrt{r_f^2 - \frac{s_F^2}{4}} & r_b > r_F \end{cases} \quad (23)$$

$$h_i = \frac{hs_F - h_r s_k}{s_F - s_k} \quad (24)$$

$$h = \sqrt{r_a^2 - \frac{s_k^2}{4}} - \sqrt{r_f^2 - \frac{s_F^2}{4}} \quad (25)$$

where d_x is the distance between the meshing point and the gear center; r_f is the effective radius of the root circle; s_k is the safety factor for tooth top bending failure.

The amount of elastic deformation of the meshing point along the line of action during meshing can be computed using the above equations. The calculation results of the involute spur gear are plotted in Fig. 8, where the modulus $m = 2$ mm, the numbers of teeth $z_1 = 35$ and $z_2 = 41$, the pressure angle $\alpha = 20^\circ$, the input power $P = 15$ kW, and the rotational speed $n = 1000$ r/min, whose distribution law is consistent with the conclusion elsewhere^[18]. The peak point of the total deflection curve is the maximum deformation.

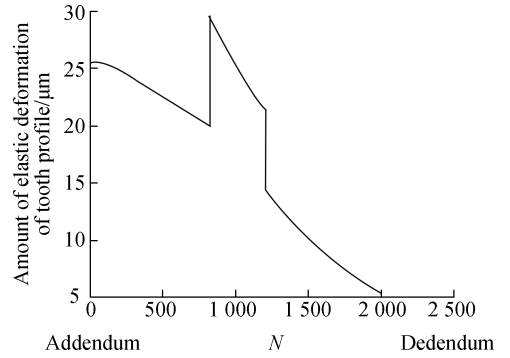


Fig. 8 Elastic deformation at each point of the tooth profile

3.2.2 Length of the modification

The length of the tip relief usually includes long and short tip reliefs. In Fig. 9, the modification area of the long tip relief is from endpoint C of the single tooth meshing area to endpoint D of the double teeth meshing area; the short tip relief has the same end as the long one, whose length is half of the long tip relief. The long tip relief is applicable for helical gears with a large helix angle and high axial contact ratio, whereas the short tip relief is more suitable for spur gears. Therefore, the sharp tip relief is used in this work.

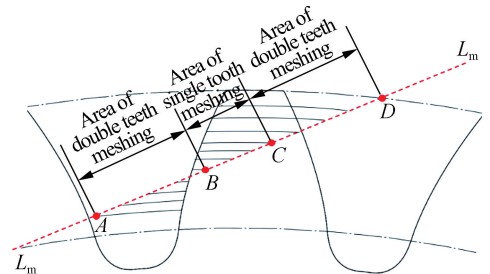


Fig. 9 Areas of the tip relief

3.2.3 Curve of modification

After the specific cutting and modification of the involute tooth profile, the curve of the tooth profile is similar to a certain curve, which is named the modification curve and mainly includes straight line and curve modifications.

The modification amount change equations for the modification curve are as follows:

For the straight-line modification, the modification amount change equation of the profile is

$$\delta_{\text{linear}} = \Delta_{\text{max}} \frac{x_{\text{sd}}}{L_d} \quad (26)$$

where x_{sd} is the distance on the meshing line from any point in the double-tooth meshing area to the point between the areas of single and double teeth, which is also termed as the relative position distance; L_d is the total length of double tooth meshing area; Δ_{max} is the maximum modification.

The curve modification primarily includes four kinds of styles: Parabolic modification, Yoshio modification, Utagawa modification, and Walker modification, whose equations of the modifications are

$$\left. \begin{aligned} \delta_{\text{Parabolic}} &= \Delta_{\text{max}} \left(\frac{x_{\text{sd}}}{L_d} \right)^2 \\ \delta_{\text{Yoshio}} &= \Delta_{\text{max}} \left(\frac{x_{\text{sd}}}{L_d} \right)^{1.22} \\ \delta_{\text{Utagawa}} &= \Delta_{\text{max}} \left[0.44 \left(\frac{x_{\text{sd}}}{L_d} \right) + 0.56 \left(\frac{x_{\text{sd}}}{L_d} \right)^2 \right] \\ \delta_{\text{Walker}} &= \Delta_{\text{max}} \left(\frac{x_{\text{sd}}}{L_d} \right)^{1.5} \end{aligned} \right\} \quad (27)$$

In this study, five modification methods are utilized to calculate the tip relief of the involute spur gear, which can give more choices when using the algorithm.

From the discussion above, the three elements of the tip relief can be determined. An example of the final modification curve is shown by the red dashed line in Fig. 10.

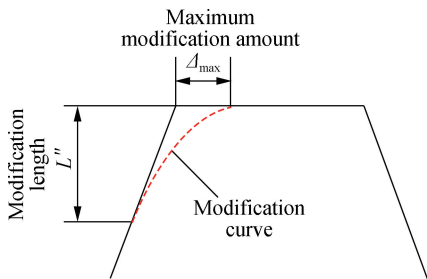


Fig. 10 Tip relief of the involute spur gear

3.2.4 Calculation results of the tip relief

The tooth profile modification equation reflects the modification amount of segmental tooth profiles; therefore, it is impossible to directly derive the function expression of the entire modified tooth profile. Thus, we obtain the function expression by curve fitting. The modification curve must meet the following three re-

quirements: ① the modification curve passes through the starting point of the double tooth meshing area; ② at the starting point of the modification curve, the curvature of the modification curve is equal to that of the involute; ③ the modification curve passes through the meshing point of the end of the tooth tip. A curve that meets the above requirements can ensure the integrity and smoothness of the tooth profile. The tip relief results from the five different modification methods are plotted in Fig. 11.

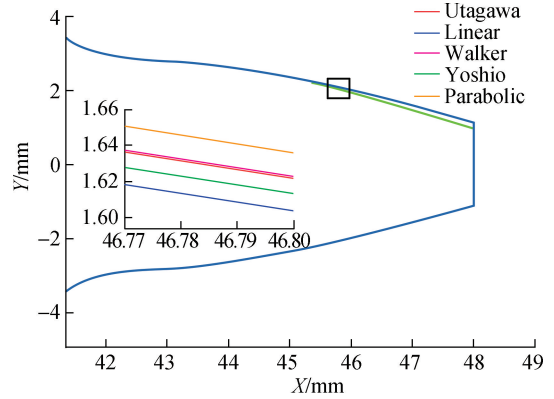


Fig. 11 Results of the tip relief method

After obtaining the modified driving gear's tooth profile coordinate point value, the curvature radius of each point of the tooth profile can be calculated. Furthermore, the curvature radius of the tooth profile of the driven gear can be calculated using the Euler-Savary equation, and the curvature radius of the tooth profile is illustrated in Fig. 12. The load distribution coefficient along the direction of the tooth profile before and after the modification is demonstrated in Fig. 13.

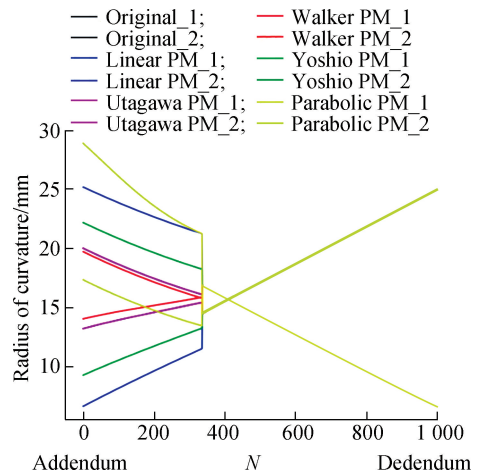


Fig. 12 Curvature radii of the modified tooth profiles

After applying the load, the stress results of the application of the five methods above are calculated, and the contact stress of the involute tooth profile after five modifications is finally output, as shown in Fig. 14. The

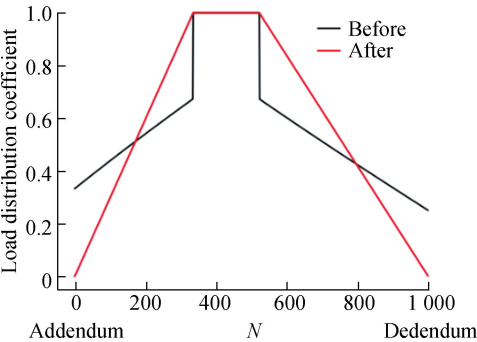


Fig. 13 Load distribution coefficients before and after tooth profile modification

contact stress curves of the tooth profiles after the modification are presented in Fig. 14(a). There is no obvious sudden change point in the stress curve, and the stress changes stably in the meshing circle. The stress difference between the unmodified and modified tooth profiles is exhibited in Fig. 14(b).

Moreover, the solution results of the contact stress can be visualized. The calculation results of the modification method selected based on the needs can be presented in a stress contour. The contours of the contact stress before and after tooth profile modification are exhibited in Fig. 15. The name of the modification method is shown at the

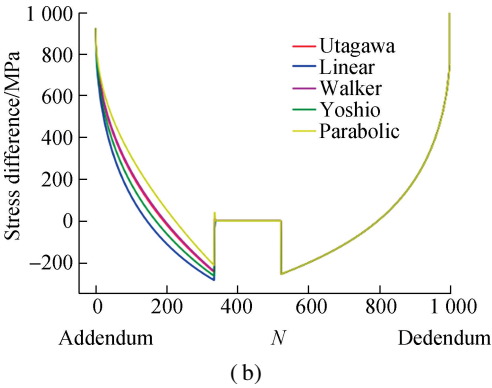
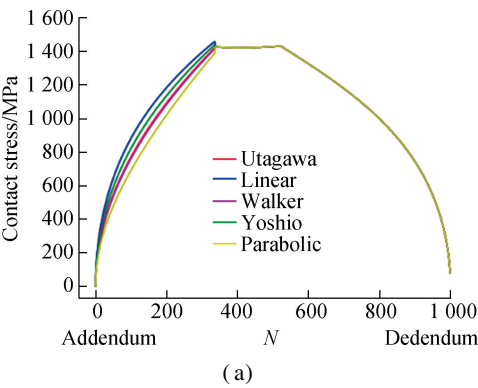


Fig. 14 Comparison of contact stress before and after tooth profile modification. (a) Contact stress after modification; (b) Stress difference between unmodified and modified tooth profiles

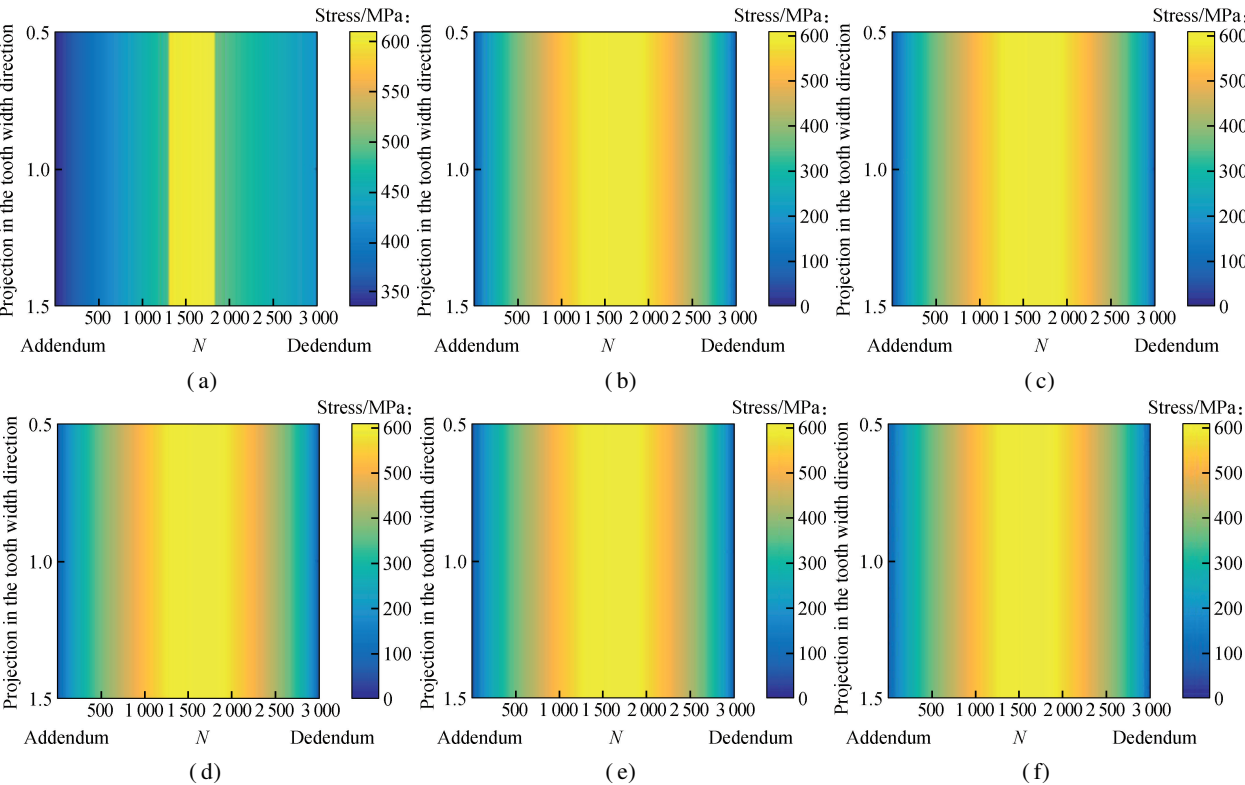


Fig. 15 Comparison of contact stress before and after tooth profile modification. (a) Before profile modification; (b) After linear profile modification; (c) After Yoshio profile modification; (d) After Utagawa profile modification; (e) After Walker profile modification; (f) After Parabolic profile modification

top of the contours, and the modified tooth profile curve equation in Fig. 15 as follows: (b) $-0.028123x^2 + 2.6204x - 57.7185 = 0$; (c) $-0.028996x^2 + 2.714x - 60.2325 = 0$; (d) $-0.030098x^2 + 2.833x - 63.4356 = 0$; (e) $-0.030047x^2 + 2.8273x - 63.2743 = 0$; and (f) $-0.031649x^2 + 3x - 67.9276 = 0$.

4 Testing and Evaluation of the Algorithm

4.1 Comparison of the contact analysis accuracy of involute spur gears

MASTA is a commercial software program for designing and analyzing gear transmission systems, which can be utilized to design and develop different gear transmission systems. The current international mainstream software MASTA, developed by SMT, is used to conduct

contact analysis of the involute spur gears. The contact analysis results are presented in Figs. 16 and 17, where the modulus $m = 3$ mm, the numbers of teeth $z_1 = 35$ and $z_2 = 41$, the pressure angle $\alpha = 20^\circ$, the tooth width $b = 30$ mm, the clearance coefficient $c^* = 0.25$, the addendum coefficient $h_a^* = 1$, Poisson's ratio $\nu = 0.3$, the elastic modulus $E = 205$ GPa, the input power $P = 20$ kW, the density $\rho = 7800$ kg/m³, and the rotational speed $n = 1600$ r/min. Here, the element type is a hexahedral element for structural analysis, and the element size is defined in MASTA as follows: mesh density on the body is 10, mesh density on the face is 8, mesh density on a fillet is 7, mesh density on the profile is 4, and mesh density on the tip is 4.

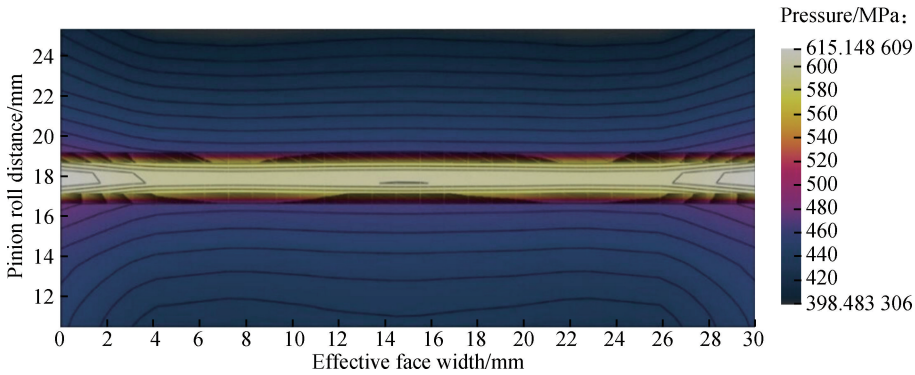


Fig. 16 Contact stress distribution in MASTA

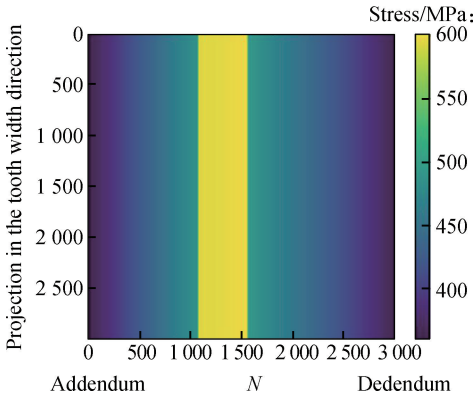


Fig. 17 Contact stress distribution with the developed algorithm

As shown in Figs. 16 and 17, comparing the maximum contact stress (609.9 MPa) calculated with the developed algorithm and that (615.1 MPa) in MASTA, the relative error is approximately 0.85%. This exhibits that the contact stress distribution with the algorithm is consistent with the MASTA result. Without pre- and post-processing operations, the basic parameters and operating condition coefficients of the gears are only input, where the contact analysis based on the Hertz formula and the modification design can be completed quickly.

4.2 Influence of transmission parameters on the accuracy of contact calculations

To further examine the calculation accuracy of the contact stress of involute cylindrical gears using the developed calculation method, the basic parameters and working condition coefficients of 168 sets of different gears are compared with the MASTA calculation results. The distribution of the error of the contact stress calculation results of the method is investigated from the three dimensions of basic parameters (such as modulus, tooth width, number of teeth, and power), contact stress, and relative error. Figs. 18 (a)-(d) are analyzed, where the hollow circle means an error within 10%, a cross means an error of less than 20%, and an asterisk means an error outside of 20%.

By comparing the calculation results of this method with the MASTA calculation results, it can be seen that when the gear modulus is small, the calculation error fluctuates to a certain extent. Nevertheless, the error is controlled within 10%. When the tooth width is large, the solved contact stress value is relatively more reliable. Relatively speaking, the calculation error increases when the number of teeth is high. Regarding the overall working conditions, the solution accuracy is more stable under low power conditions. The absolute value of the relative error of these 168 sets of studies is averaged (approx-

mately 5.04%). Among them, the number of cases with a calculation error of less than 10% is 138 (approximately 82% of the total examples), and the number of cases with a calculation error of less than 15% is 153 (approx-

mately 91% of the real cases). These verification results are reliable for the contact calculation of general involute cylindrical gear transmission in engineering.

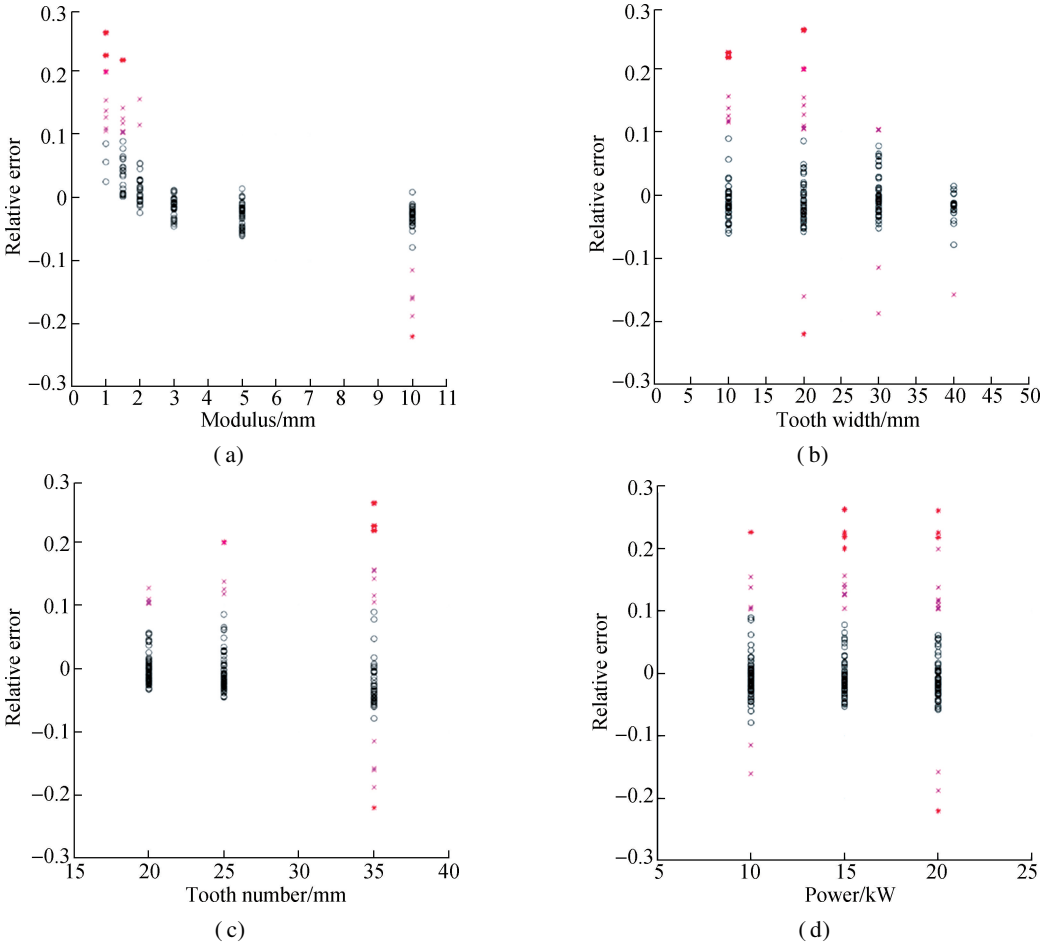


Fig. 18 Error analysis of the solution results. (a) Influence of gear modulus on solution error distribution; (b) Influence of tooth width on solution error distribution; (c) Influence of tooth number on solution error distribution; (d) Influence of power on solution error distribution

4.3 Verification of the rationality of tooth profile modification

To confirm the rationality of the tooth profile modification described in Section 3.2.4, the distribution of gear contact stress after the modification is computed and then evaluated by comparison with the MASTA results as a reference. Parabolic modification is a common tip relief

method and is more effective, especially in the case of high speed and heavy load. Thus, we use parabolic modification for verification and illustration. Using MASTA’s built-in parabolic modification function, the gear with the same parameters is modified, and the contact stress distribution is solved. The contact analysis results in the iterative process are shown in Fig. 19, and the tooth surface contact stress distribution shown in Fig. 20 is obtained.

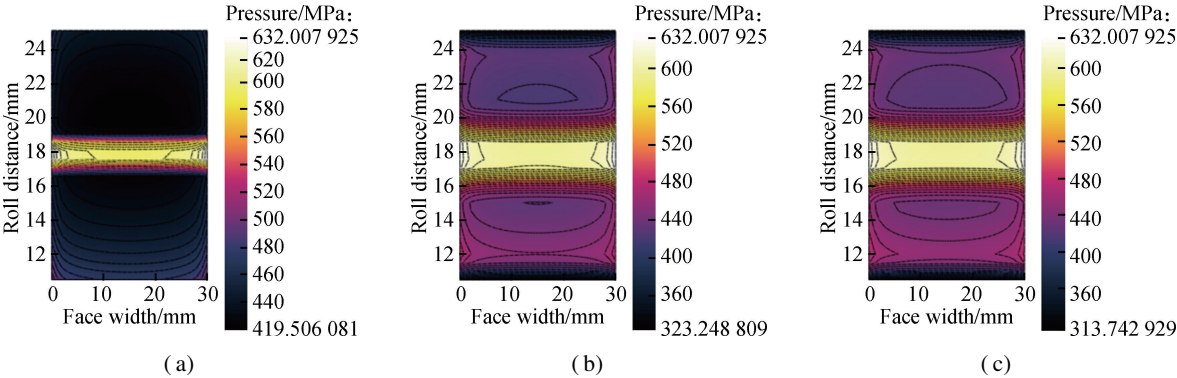


Fig. 19 Tooth profile modification iteration in MASTA. (a) Stage I; (b) Stage II; (c) Stage III

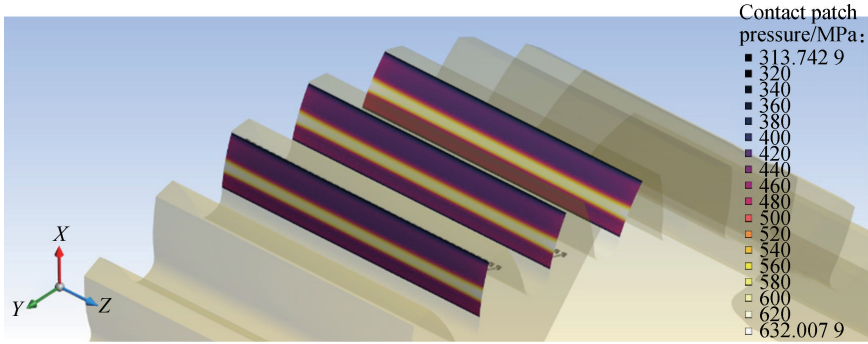


Fig. 20 Contact stress distribution after Parabolic modification in MASTA

The results of the contact stress after the designed parabolic modification are shown in Fig. 21. Because the tip relief does not change the contact stress distribution in the meshing area of a single tooth, the contact stress distribution in the meshing area remains the same as before. Because the method is based on the theoretical load distribution coefficient equation, the contact stress of the tooth tip and the part close to the tooth root, which is shown on both sides of Fig. 21 (with the modified tooth profile curve equation: $-0.031\ 649x^2 + 3x - 67.927\ 6 = 0$), is zero (means that there is no load impact of engaging in and out). MASTA is based on the finite element algorithm of Loaded Tooth Contact Analysis, and the result of contact stress is closer to the stress distribution in the actual transmission, where some sudden changes in pressure exist during engaging in and out. Overall, the results of the developed algorithm and the distribution trend of the contact stress contour have a certain calculation accuracy and rationality.

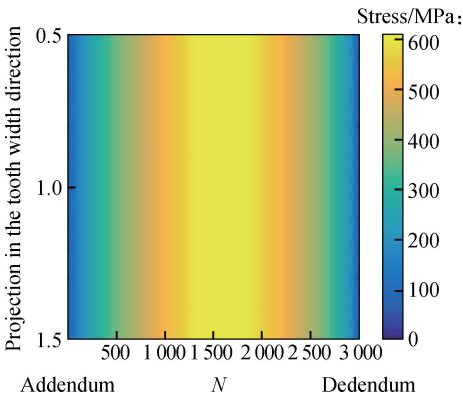


Fig. 21 Contact stress after designed parabolic modification

5 Conclusions

- 1) The mathematical model of the gear tooth profile is constructed on the basis of the forming principle of the involute tooth profile and the generating method. The involute, fillet, addendum circle, and root circle value intervals are determined by dichotomy and trichotomy. An accurate model of an involute spur gear is finally built by programming.
- 2) Based on the ISO-6336 series and the basic princi-

ples of gear transmission and load bearing, the effect of single- and double-tooth meshing on the load is analyzed. Meanwhile, the Hertz contact equation is revised by adding the load distribution coefficient and load correction coefficients. The calculation and contact stress contours of the involute spur gear are achieved using the algorithm.

3) According to the principle and methods of tooth profile modification, the equations of the amount of modification of the profile are obtained by determining the maximum amount of modification, and the contact stress distributions after modification are calculated, which completes the algorithm of tooth modification of the involute spur gear.

4) Compared with MASTA, the calculation example confirms that the error of the calculation accuracy of the contact stress of the developed algorithm is approximately 5.04%, which is close to it. Particularly, when the tooth width is large, the power and the rotational speed are low, and the algorithm results have better stability. The calculation results of the modification show that the contact stress distribution after modification is consistent with those by MASTA, which shows the rationality of the calculation results of the tooth profile modification of the developed algorithm.

Acknowledgment The authors thank the virtual laboratory at the College of Mechanical Engineering, Donghua University, for the support of the computational workstation and the software.

References

[1] Dadon I, Koren N, Klein R, et al. Impact of gear tooth surface quality on detection of local faults[J]. *Engineering Failure Analysis*, 2020, **108**: 104291. DOI: 10.1016/j.engfailanal.2019.104291.

[2] Zhai G D, Liang Z H, Fu Z H. A mathematical model for parametric tooth profile of spur gears[J]. *Mathematical Problems in Engineering*, 2020, 2020: 1–12. DOI: 10.1155/2020/7869315.

[3] Chen Z, Zeng M, Fuentes-Aznar A. Geometric design, meshing simulation, and stress analysis of pure rolling rack and pinion mechanisms[J]. *Journal of Mechanical Design*, 2020, **142** (3): 031122. DOI: 10.1115/1.

- 4044954.
- [4] Vouaillat G, Noyel J P, Ville F, et al. From Hertzian contact to spur gears: Analyses of stresses and rolling contact fatigue[J]. *Mechanics & Industry*, 2019, **20**(6): 626. DOI: 10.1051/meca/2019064.
- [5] Wen Q, Du Q G, Zhai X C. Analytical calculation of the tooth surface contact stress of spur gear pairs with misalignment errors in multiple degrees of freedom[J]. *Mechanism and Machine Theory*, 2020, **149**: 103823. DOI: 10.1016/j.mechmachtheory.2020.103823.
- [6] Sivayogan G, Rahmani R, Rahnejat H. Lubricated loaded tooth contact analysis and non-newtonian thermoelasto-hydrodynamics of high-performance spur gear transmission systems[J]. *Lubricants*, 2020, **8**(2): 20. DOI: 10.3390/lubricants8020020.
- [7] Hertz H. On the contact of elastic solids[J]. *Journal Für Die Reine Und Angewandte Mathematik*, 1881, **92**: 156 – 171.
- [8] Maper A, Karuppanan S, Patil S S. Analysis and formulation of spur gear stresses with different tip modifications [J]. *Journal of Central South University*, 2019, **26**(9): 2368 – 2378. DOI: 10.1007/s11771-019-4180-x.
- [9] Pleguezuelos M, Sánchez M B, Pedrero J I. Control of transmission error of high contact ratio spur gears with symmetric profile modifications[J]. *Mechanism and Machine Theory*, 2020, **149**: 103839. DOI: 10.1016/j.mechmachtheory.2020.103839.
- [10] Kimiaei M, Akbarzadeh S. Effect of profile modification on the performance of spur gears in isothermal mixed-EHL regime using load-sharing concept[J]. *Proceedings of the Institution of Mechanical Engineers, Part J: Journal of Engineering Tribology*, 2019, **233**(6): 936 – 948. DOI: 10.1177/1350650118806802.
- [11] Fu Z S. *Differential geometry and gear meshing principle* [M]. Dongying: China University of Petroleum Press, 1999. (in Chinese)
- [12] Pu L G, Chen G D, Wu L Y. *Machine design* [M]. 10th ed. Beijing: Higher Education Press, 2019. (in Chinese)
- [13] Wu X T. *Principle of gear meshing* [M]. Xi'an: Xi'an Jiaotong University Press, 2009. (in Chinese)
- [14] Sánchez M B, Pleguezuelos M, Pedrero J I. Enhanced model of load distribution along the line of contact for non-standard involute external gears [J]. *Meccanica*, 2013, **48**(3): 527 – 543. DOI: 10.1007/s11012-012-9612-8.
- [15] The International Organization for Standardization. Calculation of load capacity of spur and helical gears: ISO 6336-1[S]. Geneva, Switzerland: ISO copyright office, 2006.
- [16] Smith J D. *Gear noise and vibration* [M]. 2nd ed. New York, USA: Marcel Dekker, 2003.
- [17] Li R Z, Zhao Q H. *Gear strength design materials* [M]. Beijing: China Machine Press, 1984. (in Chinese)
- [18] Zhou C J, Tang J Y, Wu Y X. The comparative study of the bending stress and elastic deformation calculation of gear tooth [J]. *Journal of Mechanical Transmission*, 2004, **28**(5): 1 – 6, 65. DOI: 10.16578/j.issn.1004.2539.2004.05.001. (in Chinese)

渐开线圆柱齿轮接触分析计算与仿真研究

吕宏展 侯志勇 王君政 王羽达

(东华大学机械工程学院, 上海 201620)

摘要: 为方便实现渐开线圆柱齿轮接触分析, 开发出渐开线圆柱齿轮啮合接触分析和齿廓修形算法程序. 采用渐开线直齿轮参数方程精准建模, 获得齿廓接触点的曲率半径, 在考虑实际载荷的情况下, 改进了赫兹接触公式来求解齿轮啮合接触应力. 为减缓齿轮啮合冲击, 在算法程序中提供了 5 种齿廓修形方式及其修形后的接触应力分析方法. 与行业公认的齿轮设计仿真软件 MASTA 计算结果进行对比. 结果表明, 该算法程序接触应力求解精度较高, 相对 MASTA 平均误差约为 5.04%, 齿廓修形后的接触应力分布一致, 验证了该算法程序的合理性.

关键词: 渐开线圆柱齿轮; 赫兹公式; 接触分析; 程序开发

中图分类号: TH132